Overt visual attention modulates decision-related signals in ventral and dorsal medial prefrontal cortex

Blair R. K. Shevlin[1,2*], Rachael Gwinn[2*], Aidan Makwana[2], & Ian Krajbich[2,3,4]

[1]Center for Computational Psychiatry, Icahn School of Medicine at Mount Sinai, New York, NY, 10029

[2]Department of Psychology, The Ohio State University, Columbus, OH, 43210

[3]Department of Economics, The Ohio State University, Columbus, OH, 43210

[4]Department of Psychology, University of California Los Angeles, Los Angeles, CA, 90095

Correspondence and requests for materials should be addressed to:

Dr. Ian Krajbich

University of California Los Angeles

502 Portola Plaza

Los Angeles, CA, 90095

krajbich@ucla.edu

Conflict of Interest Statement: The authors declare no competing financial interests

Acknowledgements: Thanks to Kareem Soliman for research assistance with recruiting and to the Cattell Sabbatical Fund for financial support.

Abstract

When indicating a preference between two options, decision makers are thought to compare and accumulate evidence in an attention-guided process. Little is known about this process's neural substrates or how visual attention affects the representations of accumulated evidence. We conducted a simultaneous eye-tracking and fMRI experiment in which human subjects gradually learned about the value of two food-lotteries. With this design we were able to extend decisions over a prolonged time-course, manipulate the temporal onset of evidence, and therefore dissociate sampled and accumulated evidence. Consistent with past work, we found correlates of sampled evidence in ventromedial prefrontal cortex (vmPFC), and correlates of accumulated evidence in the prefrontal and parietal cortex. We also found that more gaze at an option increased its choice probability and that gaze amplified sampled-value signals in the vmPFC and ventral striatum. Finally, we found gaze modulated accumulated-value signals, above and beyond the non-gaze-modulated signals, in the pre-supplementary motor area (pre-SMA), providing novel evidence that visual attention has lasting effects on decision variables and suggesting that activity in the pre-SMA reflects accumulated evidence. These results shed new light on the neural mechanisms underlying gaze-driven decision processes.

Introduction

Many decisions involve a process of value computation and comparison between options. Imagine you are planning a vacation based on online travel-guides describing two locations. As you research these options, you sample pieces of information that support one option or another to varying degrees. For example, one destination might have cheaper flights while the other has cheaper hotels. Additionally, some information may attract more of your attention, such as pictures of waterfalls or ancient ruins. As you evaluate your options, you must integrate these pieces of information and eventually decide when to stop and make a final decision.

Decisions like this are thought to rely on a bounded, evidence-accumulation process that depends on factors such as the value of the sampled information and shifts in attention. According to this framework, when two options are similar in value, evidence accumulates more slowly towards the decision threshold, resulting in longer response times (RT) and more opportunity for shifts in attention to influence the choice outcome. In contrast, when one option is clearly superior, evidence accumulates more rapidly and the decision is made quickly with less of a relation between gaze and choice. This choice process produces reliable, quantitative patterns in choice, RT, and eye-tracking data (Ashby et al., 2016; Callaway et al., 2021; Gluth et al., 2018; Krajbich et al., 2010; Smith & Krajbich, 2018). For instance, decisions with similar values are more random (i.e., less predictable), tend to take more time (Konovalov & Krajbich, 2019), and can be experimentally manipulated by diverting attention towards one option more than the other (Bhatnagar & Orquin, 2022; Gwinn et al., 2019; Pärnamets et al., 2015; Pleskac et al., 2022; Tavares et al., 2017). Critically, these behavioral measures do not simply correlate; rather, they exhibit precise quantitative relationships consistent with evidence accumulation models (Konovalov & Krajbich, 2019).

Sequential sampling models (SSMs) offer a framework to understand this evidence accumulation-driven choice process. SSMs vary in specific details, but generally share some core features. When faced with a decision, people begin to sample information in favor of each option. In many models, this information is evaluated and converted into relative evidence for one option or the other. Relative evidence builds up over time until there is enough to commit to an option (Busemeyer & Townsend, 1993; Ratcliff & Smith, 2004).

Most SSMs can be broken down into two key components: inputs and integrators (Bogacz et al., 2006). Inputs encode the drift rate – the rate of evidence accumulation – and integrators encode the decision variable – the amount of accumulated evidence.

Each option has its own input. In the context of value-based decisions, the input represents the value of the currently considered piece of information. For a given option, the average input value is generally assumed to be constant over the course of the decision but does vary randomly from one instant to the next due to stochasticity in the sampling process (Shadlen & Shohamy, 2016).

Integrators accumulate the stochastic sequences of sampled input values. Typically, each option has its own integrator (Busemeyer & Townsend, 1993; Gold & Shadlen, 2007; Krajbich & Rangel, 2011; Usher & McClelland, 2001; Wang, 2002) which accumulates the evidence from that option's input, but is also inhibited by the other options' inputs or integrators. Thus, each integrator represents the accumulated, relative evidence favoring a given option. Once one of the integrators' accumulated evidence reaches a pre-determined threshold, the corresponding option is chosen. In contrast to the input values, these accumulated values dynamically evolve over the course of the decision.

The neural inputs and accumulated values have been successfully identified in perceptual decision making (for recent reviews see: Forstmann et al., 2016; Hanks & Summerfield, 2017; O'Connell et al., 2018; Ratcliff et al., 2016), but it has proven more challenging for value-based decisions. The main reason is that decisions are typically very quick, with RTs shorter than the time resolution of functional magnetic resonance imaging (fMRI) (but see Gluth et al., 2012). Evidence for the neural substrates of value-based SSMs have typically come as trial-level measures correlating with model parameters (Hare et al., 2011; Rodriguez et al., 2015), scalp-level electric activity from electroencephalography (EEG) (Polanía et al., 2014), or a combination of the two (Pisauro et al., 2017). Taken together, these studies have implicated a fronto-parietal network underlying value-based decision-making, with more ventral/frontal regions serving as inputs (for reviews see: Bartra et al., 2013; Clithero, 2018) and more dorsal/parietal regions serving as integrators.

Despite their many strengths, these past value-based experiments have been limited by their inability to determine whether purported integrator regions are accumulating evidence or instead representing unchosen values (Boorman et al., 2011; Kolling et al., 2016; Wittmann et al., 2016), decision conflict (Frömer et al., 2019; Kaanders et al., 2021; Shenhav et al., 2014, 2016; Vassena et al., 2020), or time on task (Grinband et al., 2011; Holroyd et al., 2018; Mumford et al., 2024). In most experiments, these variables are highly correlated and difficult to distinguish. Increasing the value of the worse option while holding the better option constant will simultaneously increase the perceived conflict, increase the deliberation time, and slow the rate of evidence accumulation.

To distinguish between accumulated evidence and the other confounding explanations, we sought a factor that modulates accumulated evidence within a decision, independent of time.

For this we turned to visual attention, measured with eye-tracking. Research on the attentional drift diffusion model (aDDM) has argued that gaze amplifies value during the choice process (Bhatnagar & Orquin, 2022; Krajbich et al., 2010; Sepulveda et al., 2020; Smith & Krajbich, 2019; Westbrook et al., 2020). This means that current gaze location should amplify value signals in the input regions, and that the balance of gaze allocation over the course of the decision should amplify accumulated evidence signals in the integrator regions. Both human and non-human primate research has confirmed gaze effects on value inputs in the orbitofrontal cortex (Lim et al., 2011; McGinty et al., 2016; Rich & Wallis, 2016; Hunt et al., 2018; but see McGinty, 2019). However, it has yet to be shown that these gaze-modulated inputs are integrated into accumulated decision values. Gaze modulated signals in purported integration regions would provide critical evidence against the alternative explanations (i.e., conflict, time, or unchosen value).

Here, we present the results of an fMRI experiment designed to provide evidence that integrator regions accumulate gaze-weighted evidence. Our approach was to slow down the decision process by gradually presenting choice-relevant information. Our task design allowed us to extend the decision-making period to approximately a minute, while also allowing us to dissociate the inputs' sampled value (SV) signals from the integrators' accumulated value (AV) signals (Gwinn et al., 2019). The inputs represent the perceived value of stimuli currently on the screen, while the integrators represent the values of previously presented stimuli within that choice problem. We simultaneously collected eye-tracking data, allowing us to test whether gaze modulates SV and AV representations. We specifically focus on the difference in sampled values between the left and right options (ΔSV) and the corresponding difference in accumulated values between the left and right options (ΔAV). We hypothesized that we would find (1) a positive

141 correlation between gaze-weighted $|\Delta SV|$ and activity in the reward network (the ventromedial
142 prefrontal cortex (vmPFC) and ventral striatum), and (2) a positive correlation between gaze-
143 weighted $|\Delta AV|$ in the pre-supplementary motor area (pre-SMA) (Aquino et al., 2023),
144 dorsolateral prefrontal cortex (dlPFC), and intraparietal sulcus (IPS).
145
146 **Results**
147 *Experiment description*
148 Our choice task builds on an extensive literature examining choices between familiar
149 snack foods. Instead of choosing between two food items, which typically only takes a few
150 seconds, we asked subjects to choose between two food lotteries. A lottery consisted of 3-6
151 different items, each with a different probability of being selected. Subjects did not know
152 anything else about the lotteries; they had to learn about them from experience (Hertwig et al.,
153 2004). Specifically, subjects sampled a random draw from both lotteries every 4-8 seconds. They
154 continued to sample random draws until they were ready to stop and choose one of the two
155 lotteries (Fig. 1). Choosing a lottery led to a final random draw from that lottery, revealing the
156 actual food that the subject would receive if that trial was rewarded at the end of the experiment.
157 We placed no explicit limit on the number of draws subjects could sample within each
158 trial (i.e. pair of lotteries). To prevent subjects from spending the entire session on a single trial,
159 we gave them 45 minutes to make at least 60 choices. Subjects were informed that any unmade
160 choices would be randomly completed by the computer, and any trials beyond 60 would be
161 added to the list from which the rewarded trial would be drawn. If a subject were to sample the
162 same number of stimuli in each trial, the optimal number would be seven. However, subjects
163 could (and did) vary their number of samples throughout the experiment; we observed

substantial variability in the number of samples per trial within most of our subjects (mean number of samples = 6.37 and mean within-subject *SD* = 2.61).

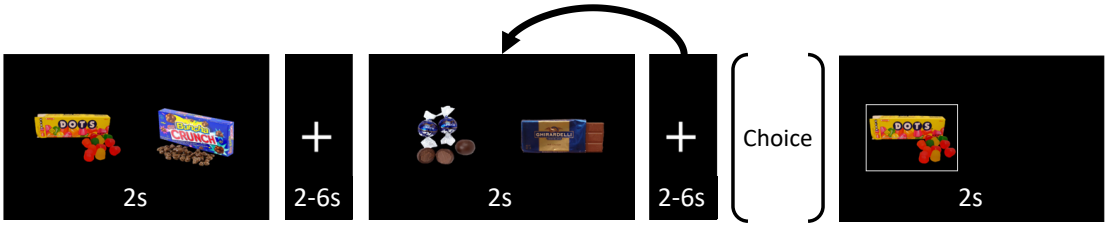

Figure 1. Task timeline. Subjects chose between two snack food lotteries on each trial. Subjects learned about the lotteries through random food draws. Every 4-8 seconds, subjects sampled a new draw from each lottery. They were allowed to sample as many times as they wanted but were incentivized to sample approximately 7 draws per trial. Sampled food draws were presented for 2 seconds, followed by a fixation cross appearing for 2-6 seconds with random jitter. The trial ended when the subject chose the left or right lottery, using the respective index finger. Upon making their choice, subjects were presented with a food drawn from their chosen lottery.

We constructed each trial's sequence of items pseudo-randomly to minimize the correlation between $|\Delta SV|$ (i.e., the absolute difference between the left and right values of the currently presented stimuli) and $|\Delta AV|$ (i.e., the absolute sum of ΔSV at a given time within a trial) (see Methods). For the first sample in each trial, ΔSV and ΔAV were always equal. After subsequent samples, ΔSV diverged from ΔAV, yielding two distinct time courses to look for in the fMRI data (Fig. 2).

To measure the subjective value of each stimulus, we separately asked subjects to rate all the food items. Before entering the scanner, subjects rated 148 unique food items based on how much they would like to eat them at the end of the experiment. These ratings were incentivized (see Methods) and we retained only the positively rated items (0 to 10) for the choice task. We used each subject's ratings to calculate SV and AV.

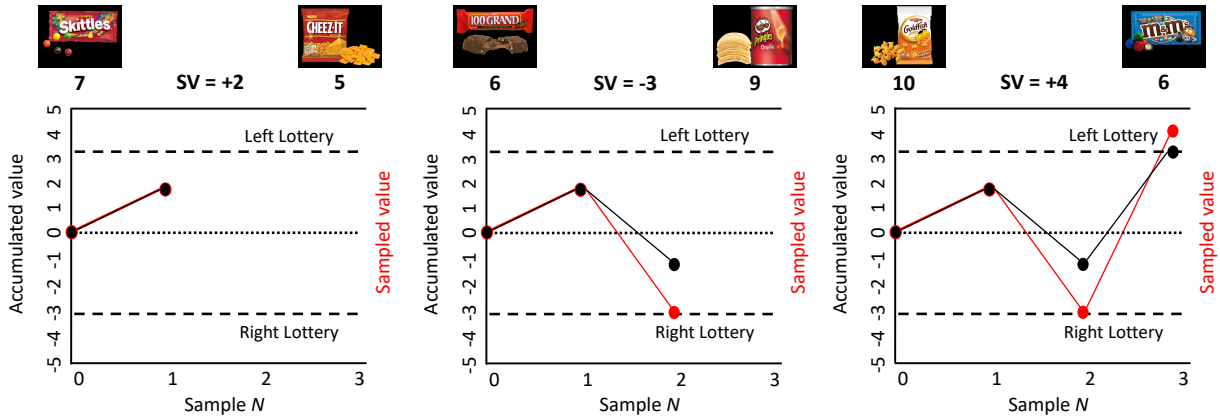

Figure 2. Example trial with the sampled value and accumulated value. The sampled value (ΔSV; red) and accumulated value (ΔAV; black) are plotted for this example trial. For the first draw, ΔSV and ΔAV are identical. However, as the trial proceeds, the two signals diverge. In the model, a choice is made when the $|\Delta AV|$ reaches a pre-specified decision boundary.

Behavioral results

A core assumption of SSMs is that individuals decide based on the evidence accumulated over the course of the decision. We thus anticipated that subjects would choose in line with ΔAV and not just the most recent ΔSV in the trial. We tested this key assumption with a mixed-effects logistic regression of choosing the left lottery on ΔSV and ΔAV at the time of choice. Subjects chose in line with both (ΔAV excluding the final samples: $\beta = 0.062$, $SE = 0.010$, $p < 0.001$; ΔSV: $\beta = 0.257$, $SE = 0.024$, $p < 0.001$) (Fig. 3A).

The larger coefficient for ΔSV compared to ΔAV is an inevitable consequence of an SSM choice process. In SSMs, a choice occurs when accumulated evidence reaches a threshold. Critically, perceived value for any given sample consists of the true underlying value plus random noise. The final sample (ΔSV) is what pushes the accumulated evidence over the threshold, which creates a selection effect: decisions tend to be made when the noise component of ΔSV is relatively large and aligned with the ultimate choice, causing the perceived final ΔSV to

systematically overestimate the true ΔSV. As a result, the regression coefficient for the effect of final ΔSV on choice is overestimated. In contrast, ΔAV represents the sum of all previous evidence, which includes samples that were insufficient to trigger a choice and thus more likely to have noise components that favored the non-chosen option. This means that the perceived ΔAV systematically underestimates the true ΔAV. As a result, the regression coefficient for the effect of ΔAV on choice is underestimated. This creates an inherent asymmetry between ΔSV and ΔAV: even when the true decision process weights evidence equally over time, regression analyses will show larger coefficients for ΔSV than ΔAV. For any data generated by an SSM, regressing choice probability on final ΔSV and total ΔAV would produce a larger coefficient for ΔSV due to this threshold-crossing selection effect.

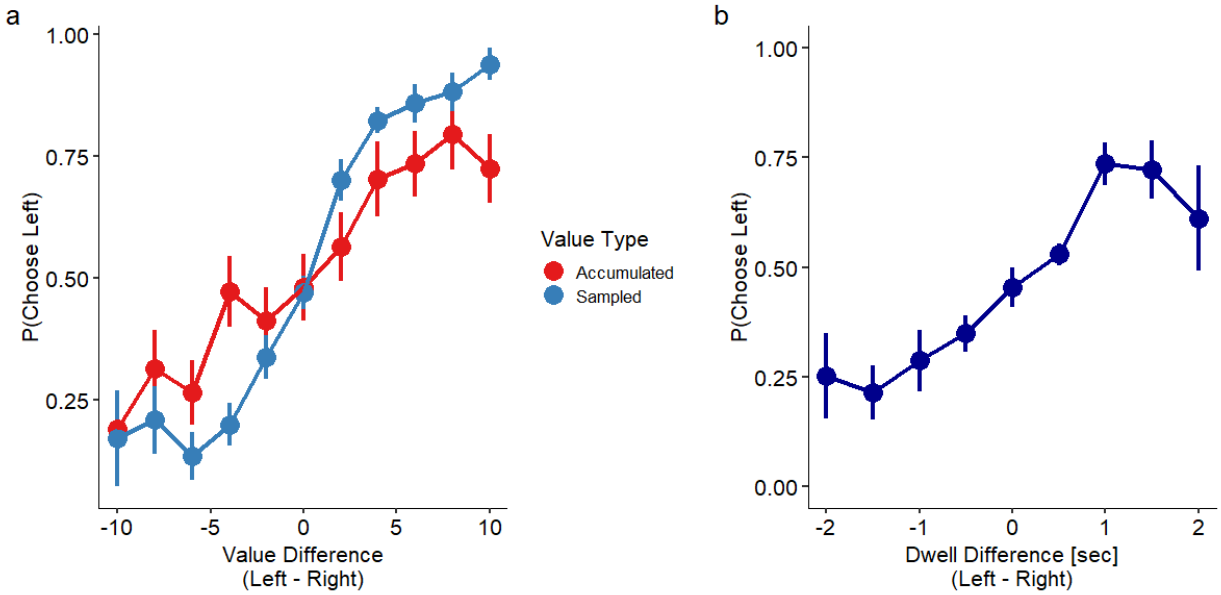

Figure 3. Choice data. (**a**) The probability of choosing left based on ΔSV and ΔAV. As the value difference becomes greater in favor of one option, the probability of choosing that option increases, for both ΔSV and ΔAV. (**b**) The effect of gaze on choice. The longer that subjects looked at one lottery over the other, over the course of the whole trial, the more likely they were to choose that lottery.

A second feature of SSM data is that easier decisions generally take less time (i.e., fewer samples). Therefore, we expected a negative correlation between the number of samples and the absolute difference in expected value between the two lotteries, as well as a higher probability of terminating a trial when the absolute value difference ($|\Delta AV|$) is higher. A mixed-effects regression of log(n samples) on the absolute expected value difference between the two lotteries revealed a negative relationship (β = -0.025, SE = 0.009, p = 0.006, two-sided t-test). A mixed-effects logistic regression of P(stop sampling) on $|\Delta AV|$ also revealed a significant positive relationship (β = 0.062, SE = 0.009, p < 0.001, two-sided t-test). These tests confirm that our subjects were sampling more in more difficult trials.

A third behavioral pattern predicted by the aDDM and other gaze-based SSMs is that individuals should generally choose options that they have looked at more (Cavanagh et al., 2014; Krajbich et al., 2010; Shimojo et al., 2003; Thomas et al., 2019; Westbrook et al., 2020). We thus anticipated a positive correlation between choice and relative dwell time over the course of the whole trial. We added dwell proportion advantage (left – right dwell time divided by total dwell time) to the choice regression and observed a positive effect on choosing the left lottery (β =1.642, SE = 0.459, p < 0.001).

To be certain that gaze-weighted evidence accumulated over the course of the whole trial, and not simply on the final sample of the trial, we excluded the final sample from each trial and re-ran the previous regression. All regressors were significant and positive (ΔSV: β = 0.290, SE = 0.028, p < .001; ΔAV: β = 0.059, SE = 0.011, p < 0.001; dwell proportion advantage: β = 1.636, SE = 0.462, p < 0.001). Thus, the influence of dwell time on choice occurred over the course of the entire decision, not simply on the final sample (Fig. 3B).

Neuroimaging results

Main analysis: Gaze-based contributions to sampled and accumulated evidence (GLM1)

Our general strategy for the fMRI data was to identify regions with BOLD activity correlating with the time series of $|\Delta SV|$ or $|\Delta AV|$. We primarily focused on the absolute value differences since we were looking for evidence in favor of making any choice, not specifically the left or right choice. This way we could identify the key components of the SSM choice process: the inputs and the integrators. We then tested whether these representations were modulated by gaze.

We tested the following hypotheses: (1) vmPFC and striatum contain input but not integrator representations; (2) the pre-supplementary motor area (pre-SMA), the intraparietal sulci (IPS), and dorsolateral PFC (dlPFC) contain integrator but not input representations; (3) the vmPFC and striatum input representations are modulated by gaze; (4) the pre-SMA, IPS, and dlPFC integrator representations are modulated by accumulated gaze.

To test all four hypotheses, we constructed a general linear model (GLM1) that included both non-gaze-weighted terms ($|\Delta SV|$ and lagged $|\Delta AV|$) and gaze-weighted terms ($|\Delta SV_{Gaze}|$ and lagged $|\Delta AV_{Gaze}|$). For hypotheses (1) and (2), the variables of interest were absolute sampled value difference ($|\Delta SV|$) and absolute accumulated value difference ($|\Delta AV|$) where $|\Delta AV| = |\sum_{t=1}^{T-1} \Delta SV_t|$, t is in units of draws (i.e., pairs of samples), and T is the current draw. Note again that we sum $|\Delta AV|$ to T-1 in order to exclude the current sample.

For hypotheses (3) and (4), the variables of interest were absolute gaze-weighted sampled values ($|\Delta SV_{Gaze}|$) and absolute gaze-weighted accumulated values ($|\Delta AV_{Gaze}|$). The sampled gaze-weighted values (ΔSV_{Gaze}) were derived by multiplying the proportion of left gaze time with the left value, and the proportion of right gaze time with the right value, within a sample.

Accumulated gaze-weighted value differences (ΔAV_{Gaze}) were the sums of ΔSV_{Gaze} across samples. Again, $|\Delta AV_{Gaze}|$ did not include the current sample.

These regressors were interacted with boxcar functions covering each sample period (2 seconds). In addition to the regressors of interest, GLM1 contained a stick function for the button press onset, modulated by lagged $|\Delta AV|$, as a nuisance regressor event, as well as a boxcar function during the feedback screen, modulated by the value of the received item. We also added motion parameter time series to account for variation due to motion. We report results using FWE-corrected statistical significance of $p < 0.05$ and a cluster significance threshold of $p < 0.005$.

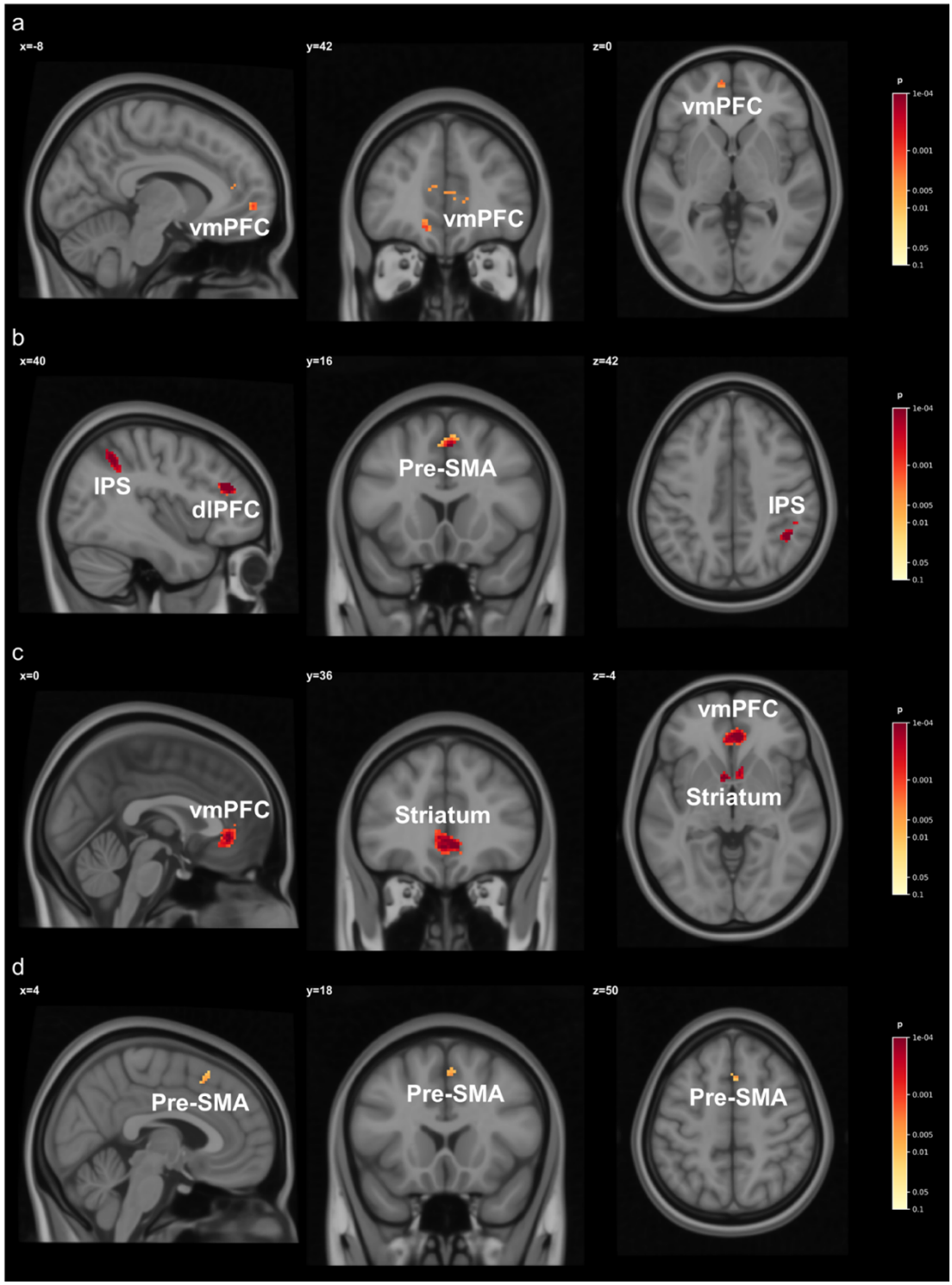

Figure 4. Regions responding to sampled value, accumulated value, and their gaze-weighted variants. (a) vmPFC showed a significantly positive correlation with $|\Delta SV|$. (b) Pre-SMA, IPS, and dlPFC showed significantly positive correlations with lagged $|\Delta AV|$. (c) vmPFC and striatum showed significantly positive correlations with $|\Delta SV_{Gaze}|$, as did pre-SMA, IPS, and dlPFC (not pictured). (d) Pre-SMA showed a significantly positive correlation with lagged $|\Delta AV_{Gaze}|$.

Hypothesis 1: vmPFC and striatum represent sampled but not accumulated value

We first investigated the vmPFC and striatum, regions that we hypothesized represent the inputs (i.e., SV). Looking specifically at BOLD activity in the vmPFC ROI defined in Bartra et al. (2013), we found a positive correlation with $|\Delta SV|$ (peak voxel x = -14, y = 44, z = -12; t = 3.90, p = 0.019) (Fig. 4A, 5A). However, we found no significant correlation with $|\Delta AV|$ in the vmPFC (Fig. 5A). The striatum showed no significant relationship with either $|\Delta SV|$ or $|\Delta AV|$ (Fig. 5A).

Hypothesis 2: pre-SMA, IPS, and dlPFC represent accumulated but not sampled value

We next investigated the pre-SMA, IPS, and dlPFC regions, which we hypothesized represent the integrated values (i.e., AV). In the pre-SMA, whose ROI we defined based on Hare et al. (2011), we found a significant, positive relationship between BOLD activity and $|\Delta AV|$ (peak voxel: x = 4, y = 14, z = 50; t = 4.75, p < 0.001) (Fig 4B, 5A), but no relationship with $|\Delta SV|$ (Fig. 5A). In the IPS, identified with the Harvard-Oxford Cortical Structural Atlas, we also saw a significant increase in activity as $|\Delta AV|$ increased (peak voxel: x = 42, y = -50, z = 42; t = 5.16, p = 0.010) (Fig. 4B, 5A), but no relationship with $|\Delta SV|$ (Fig. 5A). In the dlPFC, whose ROI we defined based on Hare et al. (2011), we found the same pattern as the pre-SMA: there was a significantly positive relationship between BOLD activity and $|\Delta AV|$ (peak voxel: x = 40, y = 34, z = 26; t = 6.83, p < 0.001) (Fig. 4B, 5A), and no relationship between BOLD activity and $|\Delta SV|$ (Fig. 5A).

In summary, we found evidence that the vmPFC represents inputs but not integrators, while the pre-SMA, IPS, and dlPFC represent integrators but not inputs.

Hypothesis 3: vmPFC and striatum sampled value representations are modulated by gaze

Having identified input and integrator regions, we next asked whether the activity in these regions was affected by gaze. The aDDM (and other gaze-weighted SSMs) predict that gaze to one option should amplify that option's value relative to the other option (Krajbich et al., 2010; Thomas et al., 2019; Westbrook et al., 2020). Consider a simple model where an option's value is weighted by the proportion of time during which it is looked at. Imagine two trials with the same pair of values, 7 on the left and 3 on the right. In Trial A, the subject looks left 30% of the time and right 70% of the time. In Trial B, the subject looks left 70% of the time and right 30% of the time. In Trial A, the net input value ("drift rate") would be $|0.3 \cdot 7 - 0.7 \cdot 3| = 0$. In Trial B, the drift rate would be $|0.7 \cdot 7 - 0.3 \cdot 3| = 4$. In Trial A, the value advantage for the left option is canceled out by the gaze advantage for the right option. In Trial B, both the value and gaze advantage favor the left option, leading to strong evidence in favor of a left choice. In sum, there is stronger evidence when gaze difference is aligned with value difference. This should be true for both ΔSV and ΔAV, though ΔSV is only affected by gaze during the current draw, while ΔAV is affected by gaze over the entire trial.

In the vmPFC, we found a significant correlation with $|\Delta SV_{Gaze}|$ (peak voxel: x = 4, y = 38, z = -4; t = 5.21, p = 0.004) but no effect of $|\Delta AV_{Gaze}|$ (Fig. 4C, 5B). Notably, the striatum also showed a significant correlation with $|\Delta SV_{Gaze}|$ (peak voxel: x = 22, y = 20, z = -10; t = 5.10, p = 0.014) (Fig. 4C, 5B), but no corresponding effect for $|\Delta AV_{Gaze}|$ (Fig. 5B). This result is particularly important because the striatum did not show sensitivity to non-gaze-weighted $|\Delta SV|$, suggesting that gaze modulation reveals striatal involvement in value processing that would otherwise be obscured.

Beyond these hypothesized relations, we also observed significant correlations between $|\Delta SV_{Gaze}|$ and activity in the IPS (peak voxel: x = -14, y = -54, z = 48; t = 4.64, p = 0.026), pre-SMA (peak voxel: x = 6, y = 6, z = 58; t = 3.33, p = 0.031), and dlPFC (peak voxel: x = 46, y = 26, z = 14; t = 3.89, p = 0.034) (Fig. 5B). This is likely due to ΔSV contributing to the accumulated evidence, which would explain activity in the purported $|\Delta AV|$ regions. In other words, there is no reason why activity in accumulator regions should only reflect the lagged $|\Delta AV|$ variable and not the most recent evidence as well.

Hypothesis 4: pre-SMA, IPS, and dlPFC accumulated value representations are modulated by gaze

In the pre-SMA we found a significantly positive relationship with $|\Delta AV_{Gaze}|$ (peak voxel: x = 4, y = 18, z = 50; t = 2.98, p = 0.032) (Fig. 4D, 5B). The IPS and dlPFC, on the other hand, did not show significant correlations with $|\Delta AV_{Gaze}|$ (Fig. 5B).

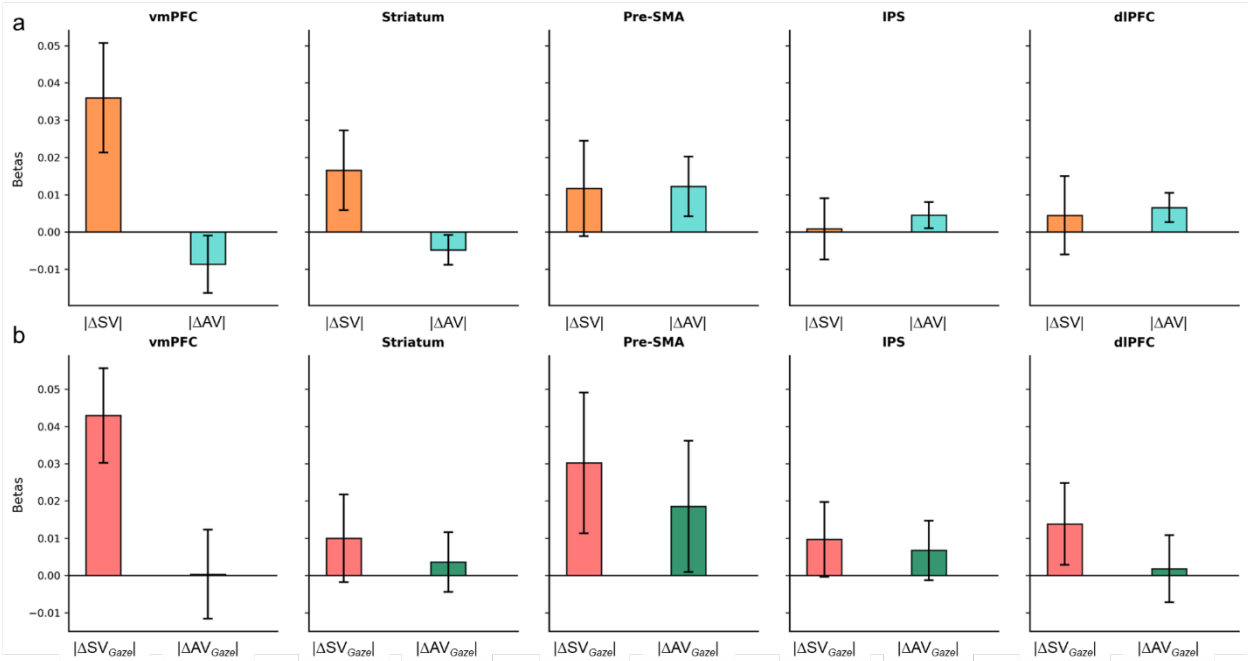

Figure 5. GLM1 beta plots from the vmPFC, striatum, pre-SMA, IPS, and dlPFC. Displayed are regression coefficients from each region for (a) non-gaze-weighted signals: absolute sampled value difference ($|\Delta SV|$) and absolute lagged accumulated value difference ($|\Delta AV|$), and (b) gaze-weighted signals: gaze-weighted sampled value ($|\Delta SV_{Gaze}|$) and absolute lagged gaze-weighted accumulated value ($|\Delta AV_{Gaze}|$). vmPFC shows a pattern of BOLD activity that scales positively with both $|\Delta SV|$ and $|\Delta SV_{Gaze}|$, but does not respond to $|\Delta AV|$ or $|\Delta AV_{Gaze}|$. The striatum shows sensitivity only to $|\Delta SV_{Gaze}|$. In contrast, the pre-SMA, IPS, and dlPFC show strong positive correlations between BOLD activity and $|\Delta AV|$, but minimal relation with $|\Delta SV|$. The pre-SMA additionally shows sensitivity to $|\Delta AV_{Gaze}|$, indicating that accumulated value representations in this region are modulated by the history of gaze allocation. Note: Bar heights reflect mean betas averaged across all voxels within each ROI. Statistical significance was determined using permutation tests with FWE correction, which identify spatially localized, reliable effects within each ROI. For the striatum, while $|\Delta SV|$ shows a numerically larger overall mean, only $|\Delta SV_{Gaze}|$ produced a spatially consistent cluster of voxels surviving FWE correction (118 voxels, $p = 0.010$).

Gaze allocation and value alignment (GLM2)

To more directly test whether accumulated evidence signals were modulated by accumulated gaze allocation throughout a trial, we conducted additional, exploratory analyses. Specifically, we ran a GLM that incorporated the following two terms: accumulated dwell advantage and $\Delta AV \times$ accumulated dwell advantage, in addition to ΔSV, the current gaze location, and $\Delta SV \times$ current gaze location.

We calculated accumulated dwell advantage as follows: For each sample *t*, accumulated dwell advantage is the cumulative difference in gaze allocation up to sample *t*-1, calculated as (total dwell left – total dwell right) / (total dwell left + total dwell right). This is a continuous measure from -1 (all previous gaze to right) to +1 (all previous gaze to left).

We also included the interaction between accumulated dwell advantage and ΔAV (i.e., signed accumulated evidence). This interaction term is positive when gaze is primarily to the left and left has more value or when gaze is primarily to the right and right has more value. This interaction term directly tests whether brain regions encoding accumulated evidence are modulated by the history of gaze allocation. This approach allows us to examine the interaction effect more explicitly as a separate regressor rather than having it embedded within the value calculation itself.

This GLM revealed a positive correlation between pre-SMA activity and the $\Delta AV \times$ accumulated dwell advantage term (peak voxel: x = 8, y = 10, z = 58; t = 3.01, $p = 0.026$). Surprisingly, the striatum also showed a correlation with this term (peak voxel: x = -16, y = 10, z = -6; t = 4.07, $p = 0.018$). Additionally, activity in the dlPFC was positively correlated with ΔSV (peak voxel: x = -36, y = 34, z = 22; t = 3.96, $p = 0.016$). No other ROIs showed significant relations.

This analysis provides additional evidence that the pre-SMA encodes accumulated value signals that are modulated by the history of gaze allocation.

Accounting for individual difference in attentional discounting (GLM3)

In our first set of analyses, we implicitly assumed complete discounting of non-fixated information, in contrast with previous studies that have generally found only partial discounting

397 (Krajbich et al., 2010; Sepulveda et al., 2020; Smith & Krajbich, 2019; Westbrook et al., 2020).
398 To verify that our results are robust to inter-subject variability in attentional discounting, we
399 estimated subject-level attentional discounting parameters and then re-estimated our original
400 GLM with new, recalculated gaze-weighted value regressors.

401 Following Smith, Krajbich, and Webb (2019), for each individual sample within a trial,
402 we computed:

403 $\beta = (G_{Left} \times V_{Left}) - (G_{Right} \times V_{Right})$

404 $\gamma = (G_{Right} \times V_{Left}) - (G_{Left} \times V_{Right})$,

405 where G_{Left} and G_{Right} represent the proportion of time spent gazing left versus right within that
406 specific sample, and V_{Left} and V_{Right} are the instantaneous values of the left and right options. We
407 then averaged these sample-level β and γ values across all samples within each trial to obtain
408 trial-level regressors. We then ran a mixed-effects logistic regression predicting choice (left vs.
409 right) as a function of β and γ and then calculated subject-specific values of $\theta = \gamma/\beta$. Across our
410 sample (N=20), we found mean $\theta = 0.77$ (SD = 0.21, range = 0.55–1.25).

411 Next, for the GLM, we computed θ-weighted sampled-value ($|\Delta SV_\theta|$) as:

412 $$\Delta SV_\theta = \left(\mathrm{G_{Left}} \times \left(\mathrm{V_{Left}} - \theta \mathrm{V_{Right}}\right)\right) - \left(\mathrm{G_{Right}} \times \left(\mathrm{V_{Right}} - \theta \mathrm{V_{Left}}\right)\right)$$

413 Similar to the original GLM, we computed an accumulated value signal, $|\Delta AV_\theta|$, based on the
414 lagged sum of previous samples' $|\Delta SV_\theta|$.

415 We found significant positive effects of $|\Delta SV_\theta|$ in the vmPFC (peak voxel: x = -14, y =
416 44, z = -12; t = 3.57 $p = 0.027$) and IPS (peak voxel: x = 30, y = -28, z = 40; t = 4.58 $p = 0.020$),
417 but in no other ROI.

418 In contrast, we found significant positive relationships between $|\Delta AV_\theta|$ and activity in the
419 pre-SMA (peak voxel: x = 0, y = 22, z = 52; t = 4.68, $p = 0.001$), dlPFC (peak voxel: x = 40, y =

32, z = 26; t = 4.32, p = 0.004), and IPS (peak voxel: x = 44, y = -48, z = 42; t = 6.26, p < 0.0001). Notably, we also observed a significant relationship between $|\Delta AV_\theta|$ and activity in the vmPFC (x = 8, y = 38, z = 18; t = 3.89, p = 0.041). No other significant contrasts emerged.

In summary, these analyses provide additional evidence that the vmPFC encodes gaze-weighted sampled value signals and the pre-SMA encodes gaze-weighted accumulated value signals, though other correlations also emerged.

Modeling a non-uniform temporal weighting function (GLM4)

While sequential sampling models like the DDM assume equal weighting of information during evidence accumulation, other models allow for information sampled at different time points to differentially impact choice. For example, information that arrives early (i.e., primacy) or late (i.e., recency) can preferentially influence decision-making (Usher & McClelland, 2001). This could especially be the case in our task where information has to be integrated over a long period of time.

To account for temporal biases during evidence accumulation, we fit participant data with a model that incorporates primacy and recency biases into the sequential sampling process (Galdo et al., 2022; Pooley et al., 2011). Within a trial *t,* the weight of sample *i* is determined by the following temporal weighting function:

$$w_t(i) = \left[1 - \left(1 - \varepsilon_p^i\right)\left(1 - \varepsilon_r^{N_t - i + 1}\right)\right](1 - \eta) + \eta, \quad (1)$$

where ε_p and ε_r are weights on primacy and recency, respectively, η is a lower bound on the weight of any sample, and N_t is the number of samples on trial *t*.

In the context of the current experiment, we assume that decision-makers accumulate evidence (ΔAV) based on the sum of sampled evidence (ΔSV) weighted by the temporal weighting function:

$$\Delta AV_{non-uniform,t} = \sum_{N_t}^{i} w_t(i)\Delta SV_t(i). \quad (2)$$

At the time of choice, the decision-maker chooses according to the logit function:

$$P_t(\text{Left Lottery}) = \frac{1}{1+e^{-\beta\Delta AV_{non-uniform,t}}} \quad (3)$$

with inverse-temperature parameter β governing the how strongly $\Delta AV_{non-uniform,t}$ governs the selection of the higher value lottery.

For models incorporating visual attention, the only modification is to use ΔSV_{Gaze} instead of ΔSV.

Behavioral model results

We observed a substantial recency bias, with all participants showing $\varepsilon_r > \varepsilon_p$ when using ΔSV and all but one participant showing $\varepsilon_r > \varepsilon_p$ when using ΔSV_{Gaze} (Fig. 6) as inputs. Independent samples t-tests (with the Welch approximation to degrees of freedom) confirmed that participants' ε_r parameters were significantly larger than their ε_p parameters, for both ΔSV ($t(36) = 12.54, p = 10^{-14}$) and ΔSV_{Gaze} ($t(20) = 7.25, p = 10^{-6}$) inputs. Goodness-of-fit measures based on the Bayesian Information Criterion (BIC) also favored a non-uniform temporal weighting function (No gaze: BIC = 1262; Gaze: BIC = 1593) over a uniform temporal weighting function (No gaze: BIC = 1307; Gaze: BIC = 1658). However, it is worth noting that the recency bias is surely over-estimated based on our parameter-recovery exercise (Methods) and the bias introduced by allowing participants to choose when to stop collecting evidence (Discussion).

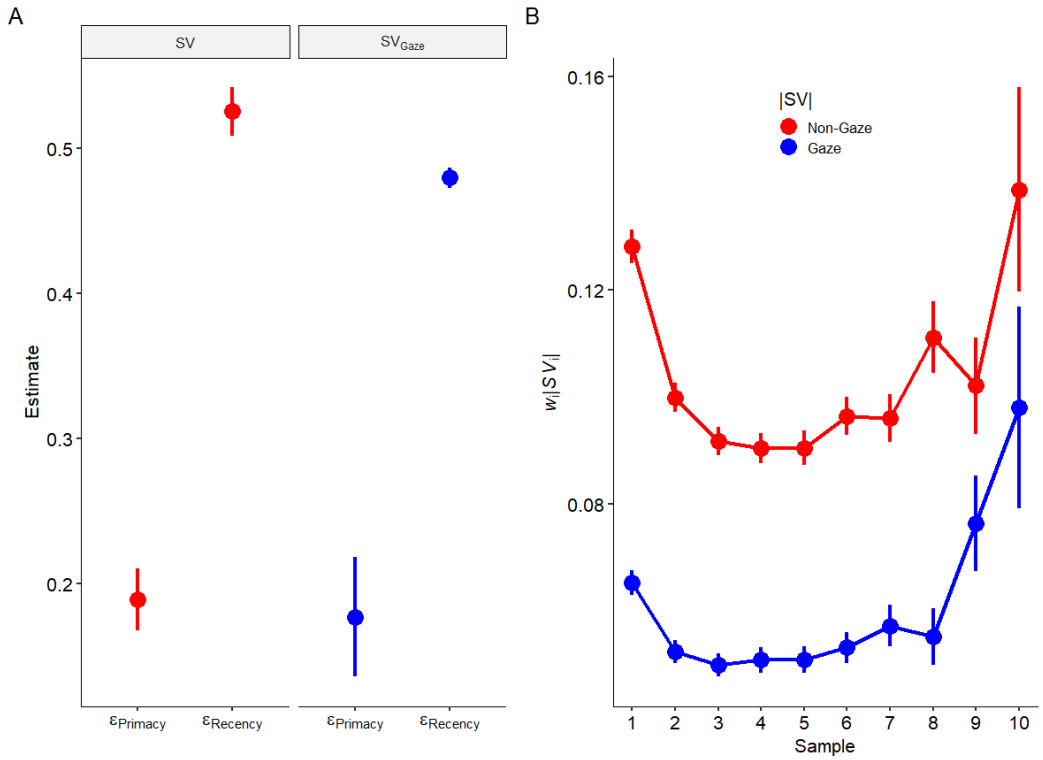

Figure 6. Non-uniform temporal weighting. In both gaze-weighted and non-gaze-weighted models, participants showed stronger recency than primacy effects, both in terms of **(A)** the model parameters, and **(B)** the resulting temporal weighting functions averaged across all trials. Error bars are standard errors clustered by participant.

fMRI model results

To identify brain regions that encoded $|\Delta AV_{non\text{-}uniform}|$, we tested whether activation parametrically varied as a function of these new values using updated versions of GLM1 in the previously defined ROIs. Within each ROI, we used a FWE corrected threshold of $p<0.05$ and cluster-forming threshold of $p<0.005$ with 5000 permutations.

We again found significant correlations between $|\Delta AV_{non\text{-}uniform}|$ and BOLD activity in the pre-SMA (peak voxel x = 0, y = 22, z = 52; t = 4.68, p = 0.001), IPS (peak voxel x = 44, y = -48, z = 42; t = 6.23, p < 0.001), and dlPFC (peak voxel x = 40, y = 32, z = 26; t = 4.32, p = 0.052).

Additionally, we found a correlation in the vmPFC (peak voxel x = 8, y = 38, z = 18; t = 3.89, p = 0.037).

For gaze-weighted $|\Delta AV_{\text{non-uniform}}|$, we found significant correlations with BOLD activity in the pre-SMA (peak voxel x = 4, y = 18, z = 50; t = 2.80 p = 0.047) and dlPFC (peak voxel x = 38, y = 30, z = 26; t = 3.86, p = 0.012).

Discussion

In this article we presented results from a simultaneous eye-tracking and fMRI study of value-based decision-making, using an expanded-judgment task where subjects sampled from, and then chose between food lotteries. We found that the vmPFC, and to a lesser extent the striatum, represent sampled input values, and the pre-SMA, IPS, and dlPFC appear to compute accumulated values. We found that sampled value signals in vmPFC and striatum are modulated by gaze allocation (Lim et al., 2011; McGinty et al., 2016), and that this gaze modulation extends to accumulated value signals in the pre-SMA.

These results provide novel evidence for the neural mechanisms underlying the SSM process, as exemplified by the DDM, which appears to govern many types of decisions (Busemeyer, 1985; Ratcliff, 1978). The gaze modulation of the accumulated value signals in the pre-SMA provides critical evidence that this region indeed represents accumulated evidence, as opposed to unchosen values (Boorman et al., 2011; Kolling et al., 2016; Wittmann et al., 2016), decision conflict (Frömer et al., 2019; Kaanders et al., 2021; Shenhav et al., 2014, 2016; Vassena et al., 2020), or time on task (Grinband et al., 2011; Holroyd et al., 2018; Mumford et al., 2024). While accumulated evidence is typically correlated with these other measures, we were able to dissociate them by taking advantage of the fact that accumulated evidence, but not the other

502 measures, are modulated by gaze location. Value is amplified by gaze (Smith & Krajbich, 2019),
503 leading to stronger value signals in the brain when the decision maker is looking at the higher
504 value option. This is what we observed in the vmPFC and striatum for input values, and in the
505 pre-SMA for accumulated values – consistent with an SSM account.

506 Conflict-based models make qualitatively different predictions. Regions implementing
507 conflict monitoring should show increased activity when options are similar in value, regardless
508 of time. The conflict account predicts that BOLD activity should scale with inverse value
509 difference: smaller $|\Delta V|$ → higher conflict → higher BOLD (Shenhav et al., 2014, 2016). In
510 simple choice tasks, high conflict and high accumulated value are both associated with long
511 response times (Pisauro et al., 2017), leading to ambiguity about how to interpret purported
512 neural correlates of accumulated value. In our task we avoided this ambiguity by analyzing the
513 effect of accumulated value at each point in time, not just at the moment of decision. With this
514 approach, conflict should be inversely correlated with accumulated value (as higher accumulated
515 evidence indicates less similarity between options). Moreover, the conflict account makes no
516 predictions about how BOLD activity should be modulated by gaze allocation for a given set of
517 option values.

518 A more serious concern is the potential confound with time-on-task BOLD activity.
519 Accumulated value inevitably increases with time within a trial, leading to a correlation between
520 the two variables (Grinband et al., 2011; Holroyd et al., 2018; Mumford et al., 2024). This is
521 where the gaze data were particularly important. Time-on-task regions should show no relation
522 with gaze allocation patterns. After accounting for non-gaze-weighted accumulated value, only
523 accumulator regions, and not time-on-task regions, should show a relationship with gaze-
524 weighted accumulated value. The results of our analyses provide exactly such evidence: pre-

525 SMA activity was positively correlated with gaze-weighted accumulated value, even when
526 accounting for previous gaze history and individual differences in attention discounting.
527 These findings were made possible by considering the role that visual attention plays in
528 the decision process. While SSMs capture choice behavior and RTs extremely well, most do not
529 consider the effects of attention. Attention is thought to shift over the course of the decision,
530 amplifying the attended inputs and/or inhibiting the non-attended inputs (Diederich, 1997;
531 Johnson & Busemeyer, 2005; Roe et al., 2001). These shifts in attention are reflected in eye-
532 movements (Hoffman & Subramaniam, 1995), which affect choice outcomes (Fiedler et al.,
533 2013; Fiedler & Glöckner, 2015; Folke et al., 2016; Glaholt & Reingold, 2009; Gwinn et al.,
534 2019; Janiszewski et al., 2013; Jiang et al., 2016; Kim et al., 2012; Konovalov & Krajbich, 2016;
535 Lopez-Persem et al., 2016; Orquin & Mueller Loose, 2013; Pärnamets et al., 2015; Polonio et al.,
536 2015; Russo & Leclerc, 1994; Sheng et al., 2020; Shi et al., 2012; Smith & Krajbich, 2018;
537 Stewart et al., 2016; Tavares et al., 2017; Towal et al., 2013; Vaidya & Fellows, 2015; Vanunu et
538 al., 2021; Venkatraman et al., 2014; J. T. Wang et al., 2010), and their effect on the choice
539 process is captured by the attentional drift diffusion model (aDDM) and other related SSMs
540 (Ashby et al., 2016; Fisher, 2021; Glickman et al., 2019; Jang et al., 2021; Krajbich et al., 2010;
541 Li & Ma, 2021; Smith & Krajbich, 2019; Teoh et al., 2020; Westbrook et al., 2020; Yang &
542 Krajbich, 2023; Zilker & Pachur, 2023).
543 Neural implementations of SSMs generally require at least two sets of neurons, one set to
544 represent the current information from the stimuli and a second set to integrate that information
545 over time. In the current study, the information being used to make decisions was subjective
546 value (i.e., utility). A large body of work has implicated the vmPFC and striatum in representing
547 value (Bartra et al., 2013; Boorman et al., 2009; Chib et al., 2009; Levy & Glimcher, 2011).

548 Interestingly, our results confirm that these two regions do represent value information, but
549 primarily just for the presented stimuli. The integrated value information, which is what
550 ultimately determines the decision, is instead encoded in the pre-SMA, IPS, and dlPFC, regions
551 that have received less attention in the literature.

552 By using eye-tracking, our study extends previous work connecting computational
553 models to fMRI data. Our results align with Hare et al.'s (2011) proposed neural model in which
554 the vmPFC provides inputs to the pre-SMA and IPS. While the Hare model was based on
555 dynamic causal modeling results, our task provides a more direct test of the proposed neural
556 network. Additionally, our eye-tracking data allows us to identify additional features of the
557 network. First, we identify the striatum as an input region, a result that only appears in analyses
558 that account for gaze-weighted value (Lim et al., 2011). Second, we find that the pre-SMA is
559 sensitive to gaze-weighted accumulated value, while the IPS is not. The reason for this
560 distinction between the pre-SMA and IPS is unclear, but it does suggest that the pre-SMA is
561 more likely to be the final decision-making region, consistent with some recent studies
562 (Juechems et al., 2017; Pisauro et al., 2017; Rodriguez et al., 2015; Rouault et al., 2019; Aquino
563 et al., 2023). Of course, the recruitment of the pre-SMA may be because our subjects made their
564 decisions with a button press, which is supported by the correlations between accumulated value
565 and motor cortex activity. Had our study required eye-movements to indicate a choice, we may
566 very well have observed integrator activity in other regions such as the frontal eye fields or
567 posterior parietal cortex (O'Connell et al., 2018).

568 A major advantage of this study is its use of a task designed to slow down the decision
569 process and force sequential integration of information. Such expanded judgment tasks have
570 been used to study SSM assumptions in perceptual decision-making, more recently in

571 combination with neural recordings, but mostly with electrophysiology in rats and monkeys
572 (Brunton et al., 2013; Cisek et al., 2009; Gluth et al., 2012; Tsetsos et al., 2012; T. Yang &
573 Shadlen, 2007).

574 On the other hand, one concern with longer decision times is that decision-makers might
575 either under-weight (i.e., forget), or put too much weight on, early information. Our analysis of
576 subjects' temporal weighting functions did reveal a primacy effect, where the first sample in
577 each trial was overweighted, as well as a recency effect, where the last samples in each trial were
578 also overweighted. Nonetheless, using a temporal weighting function with these primacy and
579 recency effects did not substantially change the conclusions from our fMRI analysis. While these
580 analyses did reveal weak support for accumulator dynamics in the vmPFC, these results should
581 be interpreted with caution because adding recency effects into the accumulated-value signal
582 increased the correlation between $|\Delta SV|$ and $|\Delta AV|$ from 0.12 to 0.21. Moreover, the recency
583 effect is surely overestimated due to well-known statistical artifacts (Mullett & Stewart, 2016).
584 In short, because decision-makers tend to terminate the decision process after strong pieces of
585 evidence, and because a strong piece of evidence will tend to have a large noise component,
586 information that appears at the end of a trial will appear to have a stronger influence on choices
587 than it should.

588 Another potential limitation of our study was the number of participants. While our
589 sample size of 20 subjects is modest by current neuroimaging standards, the within-subject
590 statistical power from our extended decision paradigm (~380 observations per subject),
591 combined with hypothesis-driven ROI analyses and multiple comparisons correction, provides
592 confidence in our core findings. Nevertheless, replication with larger samples would be valuable,
593 particularly for more fully characterizing null effects and marginal findings.

Taken together, we separated sampled input values from the overall decision value, or accumulated value, and found a network of brain regions that are involved in an aDDM-like choice process. This process involves passing sampled input values to an integrator which responds to not only the values themselves, but also to the gaze-modulated values. These results indicate that gaze effects on value representations are not epiphenomenal; rather, they reflect how gaze is incorporated into the decision process, affecting how we perceive the value of each option over the course of the entire decision.

Materials and Methods

Experimental Design and Statistical Analyses

Subjects

Twenty-eight undergraduate students at The Ohio State University participated in this study. Due to time constraints, 4 subjects were unable to finish all 3 runs of the scan. One subject was excluded for not choosing in line with their ratings. This left 23 subjects in the analysis (14 men, 9 women, average age: 22.61). Another 3 subjects could not be calibrated on the eye-tracker and so are discarded from any analyses involving eye tracking (leaving 13 men, 7 women, average age: 22.9). All subjects were right-handed, had normal or corrected-to-normal vision, and no history of neurological disorders. This study was approved by The Ohio State Biomedical Sciences IRB.

Stimuli and Tasks

Rating Task: Outside of the scanner, subjects rated 148 food items using a continuous rating scale from -10 (extreme dislike) to 10 (extreme like), with 0 being indifference towards an item. To choose their preferred rating, subjects moved the mouse across the rating scale and then

clicked the left mouse button when the cursor was at their desired value for the item. We used an incentivization procedure for these ratings. There was a 50% chance that the rating task would be used to determine the subject's reward. In such cases, the computer would randomly select two foods and the subject would receive the one with the higher rating. If both items were rated negatively, the subject would not receive any food. Negative values (-10 to 0) were excluded from the choice task except for two subjects who did not have enough positively valued items.

Choice Task: Once in the MRI scanner, subjects chose between pairs of lotteries. Lotteries were constructed by creating 1000 potential lotteries of randomly selected items evenly split between having 3, 4, 5, or 6 items. Each item in a lottery was then assigned a probability of being drawn, with probabilities summing up to 1 in each lottery. For each of these lotteries we calculated its expected utility by multiplying the subjective value (i.e., rating) of each item (V_i) in the lottery by its associated probability (P_i) of being drawn, and summing the results

$$EU = \sum_{i=1}^{N} P_i * V_i \quad (4)$$

where N is the total number of items in that lottery. Subjects were not told these probabilities, nor were they told which items were in each lottery – they had to learn this every trial.

We tracked subjects' eye movements in the scanner using an Eyelink 1000 plus (SR Research) set at 500 Hz. Eye position was monitored with the camera and infrared source reflected in the mirror attached to the head coil. The eye tracker was calibrated at the beginning of the session.

Food items were sampled from the lotteries and presented on the screen one pair at a time. Each draw was presented for 2 seconds, followed by a fixation cross for 2-6 seconds. This process repeated until the subject made a choice. Once a subject was ready to choose a lottery,

they used the index finger of their left (right) hand to press a button corresponding to the left (right) lottery. They were then presented with a random item from the lottery they had chosen (on the same side of the screen as the chosen basket) for 2 seconds, indicating the food they would receive from this trial, should it be randomly selected at the end of the study (Fig. 1).

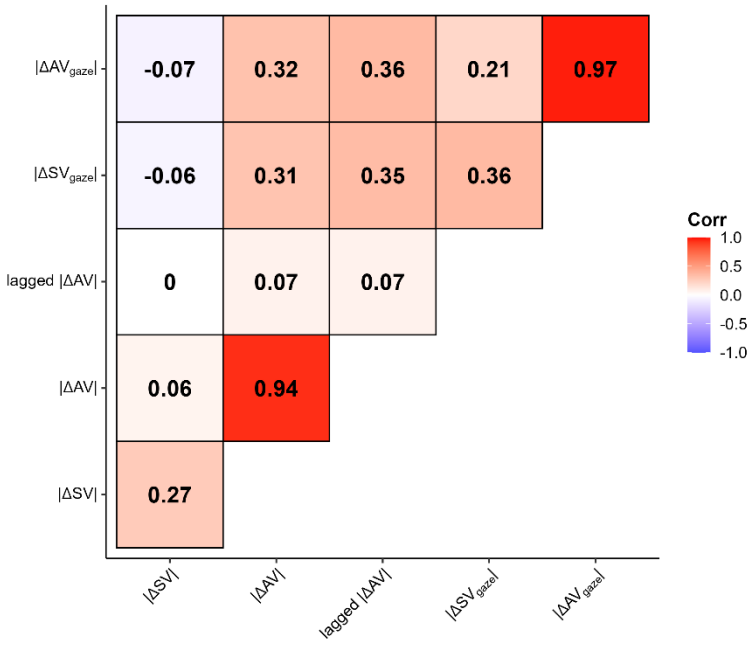

Figure 7. Sample-level correlations between value signal regressors. Pearson correlations computed across samples for different quantifications of sampled value (ΔSV) and accumulated value (ΔAV). Values represent correlations between absolute magnitudes of each measure. $|\Delta SV|$ = absolute sampled value difference; $|\Delta AV|$ = absolute accumulated value difference; lagged $|\Delta AV|$ = absolute accumulated value difference up to the previous sample; $|\Delta SV_{Gaze}|$ = gaze-weighted sampled value; $|\Delta AV_{Gaze}|$ = gaze-weighted accumulated value; lagged $|\Delta AV_{Gaze}|$ = gaze-weighted accumulated value from the previous sample.

We constructed each trial's sequence of items pseudo-randomly to minimize the correlation between the sampled value signal ($|\Delta SV|$; i.e., the absolute difference in sampled input values) and the accumulated value signal ($|\Delta AV|$; i.e., the absolute difference in accumulated values). For the first draw in each trial, sampled and accumulated value signals are equal. On

subsequent draws, the $|\Delta SV|$ diverges from the $|\Delta AV|$ signal, yielding two distinct time courses to look for in the fMRI data (Fig. 2). Across subjects, $|\Delta SV|$ and $|\Delta AV|$ had an average correlation of 0.31 (SD = 0.10, min = 0.08, max = 0.45), while $|\Delta SV|$ and lagged $|\Delta AV|$ (i.e., the variables in our GLMs) had an average correlation of 0.07 (SD = 0.08, min = -0.09, max = 0.17). See Figure 7 for the full correlation matrix of value signal regressors calculated across subjects and samples.

The task structure was designed to incentivize subjects to average 7 samples per trial. They had 45 minutes to make 60 choices, and any trials that they did not complete by the end of the experiment were made for them randomly by the computer. Any trials they completed beyond 60 were simply added to the pool of potentially rewarded trials. At the end of the study, there was a 50% chance that one of the choice trials would be randomly selected for payment (otherwise the rating task was selected for payment), in which case the subject received the corresponding food from that trial.

Outside of the scanner, subjects first completed a 5-minute practice section where they chose between baskets made up of cars. After each trial, they were given feedback on how many samples they took and were reminded that the goal was to take 7 samples on average. These choices were not incentivized.

Temporal-weighting-function model fits

We estimated model parameters using an iterative maximum a posteriori (MAP) approach (Huys et al., 2011; Wittmann et al., 2020). This method improves upon maximum likelihood estimation (MLE) by simultaneously estimating parameters at both the subject- and group-level. This hierarchical procedure constrains subject-level parameters and reduces the influence of outlier data.

Group-level parameters were initialized with uninformative Gaussian priors with mean of 0.1 and variance of 100. For all models, η was held constant at 1. During the expectation step, we estimated model parameters ($\varepsilon_p, \varepsilon_r, \beta$) for each participant using MLE and calculated the log-likelihood of their choices given the model parameters. During the maximization step, we calculated the maximum posterior probability based on the observed choices and prior group-level parameters, and then updated the group-level parameters to generate posterior parameter estimates. These posterior parameter estimates were then used as the priors in subsequent steps in this procedure. We iteratively repeated the expectation and maximization steps until convergence of the posterior likelihood summed over group-level parameters exceeded a change of less than 0.0001 from the previous iteration (for a maximum of 800 iterations). During this procedure, bounded free parameters were transformed from Gaussian space to native model space using link functions (e.g., sigmoidal function for $\varepsilon_p, \varepsilon_r$) to ensure accurate estimation near the bounds.

We assessed parameter recovery of this model on simulated choices using best-fitting model parameters. We then refit the simulated choices using the same MAP process described above. We found strong Pearson's *r* correlations between the generated and estimated parameter values ($r > .8$; Fig. 8), though both parameters were systematically over-estimated.

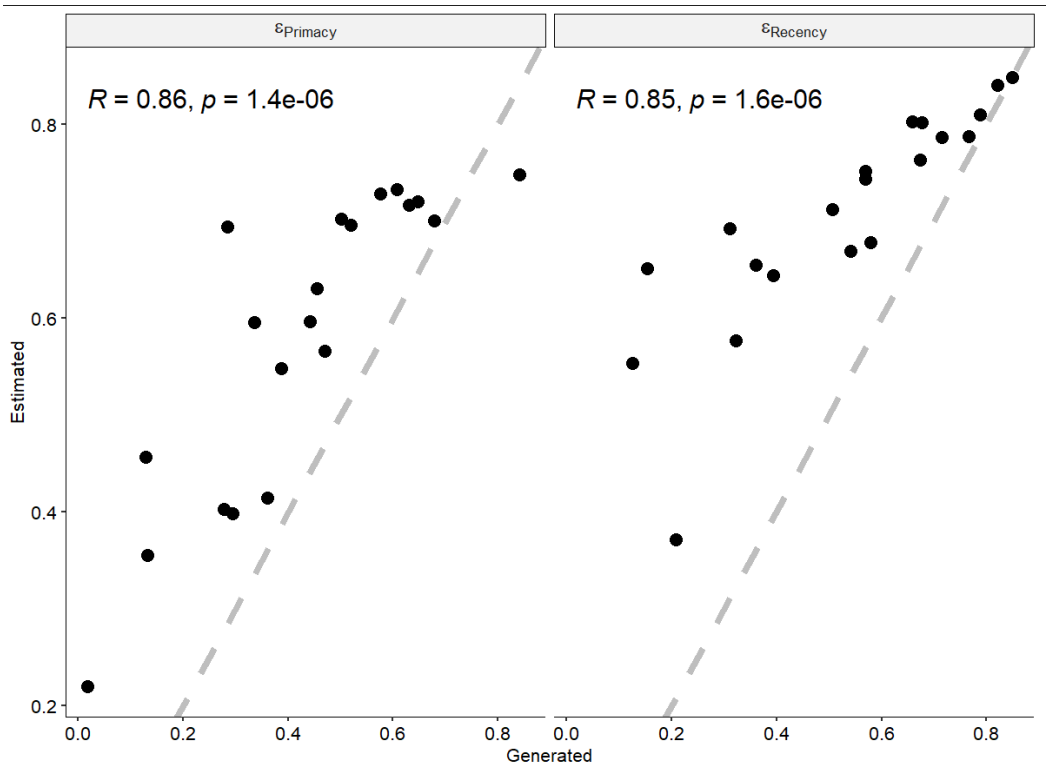

Figure 8. Correlation plots illustrating parameter recovery.

MRI Data Acquisition

MRI scanning was carried out at the OSU Center for Cognitive and Behavioral Brain Imaging. We used a 3T Siemens Magnetom Prisma scanner with a 32-channel head array coil to collect the neural data. Functional data were acquired with a T2*-weighted gradient-echo sequence (48 slices, interleaved, with a field of view of 1554x1554, with an in-plane resolution of 3 mm isotropic and a 3mm slice gap, TR = 2600 ms, TE = 28 ms, 80° flip angle). Slices were oriented such that the anterior side of the acquisition was raised dorsally by 30 degrees compared to the line formed by joining the anterior commissure to the posterior commissure. A high-resolution MPRAGE anatomical scan (256 slices, field of view 224x256, with an in-plane resolution of 1 mm and no slice gap, TR = 1900 ms, TE = 4.44 ms, 12° flip angle) was also acquired for each participant. Each participant was scanned in one 1.5-hour session, which included the three experimental runs (15 minutes each) and the high-resolution MPRAGE

anatomical scan. Additionally, a resting state scan (5 minutes) and a DTI scan were acquired, but these data are not presented here. Stimuli were presented using Psychtoolbox (Brainard, 1997; Kleiner et al., 2007; Pelli, 1997) for MATLAB (MATLAB, 2016), and displayed with a DLP projector onto a screen mounted in the rear of the scanner bore.

MRI Preprocessing and analyses

Statistical parametric mapping (SPM12, Update Rev. Nr. 6905; Functional Imaging Laboratory, University College London) was used to carry out the preprocessing of fMRI data. First, we corrected for the different slice times per echo planar image (EPI) across the total volume (using the bottom slice as a reference) and then realigned each volume in a run to the mean EPI volume from that run. Next, the anatomical scan was coregistered with the MNI average of 152 brains template, and the mean EPI per run was used to coregister all functional scans to this coregeistered anatomical scan. In order to warp the EPIs to MNI space, SPM12's *normalise* function was applied to the coregistered anatomical scan and the resulting warping parameters were applied to the coregistered EPIs. The resulting images were smoothed using an isometric Gaussian kernel (8 mm full width at half maximum). First level GLMs were run using SPM on each subject individually, including contrasts of interest. Runs were combined using *fslmerge*. We then used the Statistical non-Parametric Mapping toolbox (e.g., SnPM013.1.09) function to run second-level, non-parametric significance tests with threshold-free clustering and family wise error (FWE) correction to find significant clusters for the described effects (Nichols & Holmes, 2002). We report the results of 5000 permutations using FWE-corrected statistical significance of $p < 0.05$ and a cluster significance threshold of $p < 0.005$.

We used a canonical hemodynamic response function (HRF) without time derivatives. We modeled the noise as an AR(1) process. We additionally used a high-pass filter set to 128 s. We also used global signal normalization with a value of 0.8. We used no corrections for susceptibility distortions. All general linear models (GLM) included variants of $|\Delta SV|$ and lagged $|\Delta AV|$, either gaze weighted or not, interacted with boxcar functions covering each sample period (2 seconds) – see details below. In addition to the regressors of interest, each GLM contained the following nuisance terms: a stick function for trial number, a stick function for the button press onset modulated by lagged $|\Delta AV_{Gaze}|$, and a boxcar function during the feedback screen, modulated by the value of the received item. We also added motion parameter time series to account for variation due to motion.

In our primary analyses (GLM1), in addition to the nuisance terms, we included the following regressors: $|\Delta SV|$, lagged $|\Delta AV|$, $|\Delta SV_{Gaze}|$ and lagged $|\Delta AV_{Gaze}|$.

In our analyses of gaze allocation history (GLM2), in addition to the nuisance terms, we included the following regressors: ΔSV, lagged ΔAV, current gaze location, accumulated dwell advantage, $\Delta SV \times$ current gaze location, and lagged $\Delta AV \times$ accumulated dwell advantage.

In our analysis incorporating individual differences in attentional discount (GLM3), in addition to the nuisance terms, we included the following regressors: θ-weighted $|\Delta SV|$ and lagged θ-weighted $|\Delta AV|$.

In our analysis incorporating non-uniform temporal weighting of accumulated evidence (GLM4), in addition to the nuisance terms, we included the following regressors: $|\Delta SV|$, lagged $|\Delta AV_{non\text{-}uniform}|$, $|\Delta SV_{Gaze}|$ and lagged $|\Delta AV_{non\text{-}uniform,\ Gaze}|$.

None of the regressors in the models were orthogonalized.

Region of interest specifications

ROIs were based upon previously published brain atlas parcellations and relevant literature. We used the Harvard-Oxford atlas for the intraparietal sulcus (IPS) and striatum (Desikan et al., 2006). The dorsolateral prefrontal cortex (dlPFC) and pre-supplementary motor area (pre-SMA) were defined based on (Hare et al., 2011). The ventromedial prefrontal cortex (vmPFC) was defined in (Bartra et al., 2013).

Data Availability

Experiment and analysis code as well as Behavioral and eye-tracking data are available on the Open Science Framework: https://osf.io/eyxvb/files/

fMRI data is available on Open Neuro: doi:10.18112/openneuro.ds007305.v1.0.0

References

Aquino, T.G., Cockburn, J., Mamelak, A.N., Rutishauser, U., O'Doherty, J.P. (2023) Neurons in human pre-supplementary motor area encode key computations for value-based choice. *Nature Human Behaviour, 7*, 970–985. https://doi.org/10.1038/s41562-023-01548-2

Ashby, N. J. S., Jekel, M., Dickert, S., & Glöckner, A. (2016). Finding the right fit: A comparison of process assumptions underlying popular drift-diffusion models. *Journal of Experimental Psychology: Learning, Memory, and Cognition*, *42*(12), 1982–1993. https://doi.org/10.1037/xlm0000279

Bartra, O., McGuire, J. T., & Kable, J. W. (2013). The valuation system: A coordinate-based meta-analysis of BOLD fMRI experiments examining neural correlates of subjective value. *NeuroImage*, *76*, 412–427. https://doi.org/10.1016/j.neuroimage.2013.02.063

Bhatnagar, R., & Orquin, J. L. (2022). A meta-analysis on the effect of visual attention on choice. *Journal of Experimental Psychology: General*, *151*(10), 2265. https://doi.org/10.1037/xge0001204

Bogacz, R., Brown, E., Moehlis, J., Holmes, P., & Cohen, J. D. (2006). The physics of optimal decision making: A formal analysis of models of performance in two-alternative forced-choice tasks. *Psychological Review*, *113*(4), 700. https://doi.org/10.1037/0033-295X.113.4.700

Boorman, E. D., Behrens, T. E. J., Woolrich, M. W., & Rushworth, M. F. S. (2009). How Green Is the Grass on the Other Side? Frontopolar Cortex and the Evidence in Favor of Alternative Courses of Action. *Neuron*, *62*(5), 733–743. https://doi.org/10.1016/j.neuron.2009.05.014

Boorman, E. D., Behrens, T. E., & Rushworth, M. F. (2011). Counterfactual Choice and Learning in a Neural Network Centered on Human Lateral Frontopolar Cortex. *PLOS Biology*, *9*(6), e1001093. https://doi.org/10.1371/journal.pbio.1001093

Brainard, D. H. (1997). The Psychophysics Toolbox. *Spatial Vision*, *10*(4), 433–436. https://doi.org/10.1163/156856897X00357

Brunton, B. W., Botvinick, M. M., & Brody, C. D. (2013). Rats and humans can optimally accumulate evidence for decision-making. *Science*, *340*(6128), 95–98. https://doi.org/10.1126/science.1233912

Busemeyer, J. R. (1985). Decision making under uncertainty: A comparison of simple scalability, fixed-sample, and sequential-sampling models. *Journal of Experimental Psychology: Learning, Memory, and Cognition*, *11*(3), 538–564. https://doi.org/10.1037/0278-7393.11.3.538

Busemeyer, J. R., & Townsend, J. T. (1993). Decision field theory: A dynamic-cognitive approach to decision making in an uncertain environment. *Psychological Review*, *100*(3), 432–459. https://doi.org/10.1037/0033-295X.100.3.432

Callaway, F., Rangel, A., & Griffiths, T. L. (2021). Fixation patterns in simple choice reflect optimal information sampling. *PLOS Computational Biology*, *17*(3), e1008863. https://doi.org/10.1371/journal.pcbi.1008863

Cavanagh, J. F., Wiecki, T. V., Kochar, A., & Frank, M. J. (2014). Eye tracking and pupillometry are indicators of dissociable latent decision processes. *Journal of Experimental Psychology: General*, *143*(4), 1476–1488. https://doi.org/10.1037/a0035813

Chib, V. S., Rangel, A., Shimojo, S., & O'Doherty, J. P. (2009). Evidence for a Common Representation of Decision Values for Dissimilar Goods in Human Ventromedial Prefrontal Cortex. *Journal of Neuroscience*, *29*(39), 12315–12320. https://doi.org/10.1523/JNEUROSCI.2575-09.2009

Cisek, P., Puskas, G. A., & El-Murr, S. (2009). Decisions in Changing Conditions: The Urgency-Gating Model. *Journal of Neuroscience*, *29*(37), 11560–11571. https://doi.org/10.1523/JNEUROSCI.1844-09.2009

Clithero, J. A. (2018). Improving out-of-sample predictions using response times and a model of the decision process. *Journal of Economic Behavior & Organization*, *148*, 344–375. https://doi.org/10.1016/j.jebo.2018.02.007

Desikan, R. S., Ségonne, F., Fischl, B., Quinn, B. T., Dickerson, B. C., Blacker, D., Buckner, R. L., Dale, A. M., Maguire, R. P., Hyman, B. T., Albert, M. S., & Killiany, R. J. (2006). An automated labeling system for subdividing the human cerebral cortex on MRI scans into

gyral based regions of interest. *NeuroImage*, *31*(3), 968–980. https://doi.org/10.1016/j.neuroimage.2006.01.021

Diederich, A. (1997). Dynamic Stochastic Models for Decision Making under Time Constraints. *Journal of Mathematical Psychology*, *41*(3), 260–274. https://doi.org/10.1006/jmps.1997.1167

Fiedler, S., & Glöckner, A. (2015). Attention and moral behavior. *Current Opinion in Psychology*, *6*, 139–144. https://doi.org/10.1016/j.copsyc.2015.08.008

Fiedler, S., Glöckner, A., Nicklisch, A., & Dickert, S. (2013). Social Value Orientation and information search in social dilemmas: An eye-tracking analysis. *Organizational Behavior and Human Decision Processes*, *120*(2), 272–284. https://doi.org/10.1016/j.obhdp.2012.07.002

Fisher, G. (2021). Intertemporal Choices Are Causally Influenced by Fluctuations in Visual Attention. *Management Science*, *67*(8), 4961–4981. https://doi.org/10.1287/mnsc.2020.3732

Folke, T., Jacobsen, C., Fleming, S. M., & De Martino, B. (2016). Explicit representation of confidence informs future value-based decisions. *Nature Human Behaviour*, *1*(1), Article 1. https://doi.org/10.1038/s41562-016-0002

Forstmann, B. U., Ratcliff, R., & Wagenmakers, E.-J. (2016). Sequential Sampling Models in Cognitive Neuroscience: Advantages, Applications, and Extensions. *Annual Review of Psychology*, *67*(1), 641–666. https://doi.org/10.1146/annurev-psych-122414-033645

Frömer, R., Dean Wolf, C. K., & Shenhav, A. (2019). Goal congruency dominates reward value in accounting for behavioral and neural correlates of value-based decision-making. *Nature Communications*, *10*(1), Article 1. https://doi.org/10.1038/s41467-019-12931-x

Galdo, M., Weichart, E. R., Sloutsky, V. M., & Turner, B. M. (2022). The quest for simplicity in human learning: Identifying the constraints on attention. *Cognitive Psychology*, *138*, 101508. https://doi.org/10.1016/j.cogpsych.2022.101508

Glaholt, M. G., & Reingold, E. M. (2009). Stimulus exposure and gaze bias: A further test of the gaze cascade model. *Attention, Perception, & Psychophysics*, *71*(3), 445–450. https://doi.org/10.3758/APP.71.3.445

Glickman, M., Sharoni, O., Levy, D. J., Niebur, E., Stuphorn, V., & Usher, M. (2019). The formation of preference in risky choice. *PLOS Computational Biology*, *15*(8), e1007201. https://doi.org/10.1371/journal.pcbi.1007201

Gluth, S., Rieskamp, J., & Büchel, C. (2012). Deciding When to Decide: Time-Variant Sequential Sampling Models Explain the Emergence of Value-Based Decisions in the Human Brain. *Journal of Neuroscience*, *32*(31), 10686–10698. https://doi.org/10.1523/JNEUROSCI.0727-12.2012

Gluth, S., Spektor, M. S., & Rieskamp, J. (2018). Value-based attentional capture affects multi-alternative decision making. *eLife*, *7*, e39659. https://doi.org/10.7554/eLife.39659

Gold, J. I., & Shadlen, M. N. (2007). The Neural Basis of Decision Making. *Annual Review of Neuroscience*, *30*(1), 535–574. https://doi.org/10.1146/annurev.neuro.29.051605.113038

Grinband, J., Savitskaya, J., Wager, T. D., Teichert, T., Ferrera, V. P., & Hirsch, J. (2011). The dorsal medial frontal cortex is sensitive to time on task, not response conflict or error likelihood. *NeuroImage*, *57*(2), 303–311. https://doi.org/10.1016/j.neuroimage.2010.12.027

Gwinn, R., Leber, A. B., & Krajbich, I. (2019). The spillover effects of attentional learning on value-based choice. *Cognition*, *182*, 294–306. https://doi.org/10.1016/j.cognition.2018.10.012

Hanks, T. D., & Summerfield, C. (2017). Perceptual Decision Making in Rodents, Monkeys, and Humans. *Neuron*, *93*(1), 15–31. https://doi.org/10.1016/j.neuron.2016.12.003

Hare, T. A., Schultz, W., Camerer, C. F., O'Doherty, J. P., & Rangel, A. (2011). Transformation of stimulus value signals into motor commands during simple choice. *Proceedings of the National Academy of Sciences*, *108*(44), 18120–18125. https://doi.org/10.1073/pnas.1109322108

Hoffman, J. E., & Subramaniam, B. (1995). The role of visual attention in saccadic eye movements. *Perception & Psychophysics*, *57*(6), 787–795. https://doi.org/10.3758/BF03206794

Holroyd, C. B., Ribas-Fernandes, J. J. F., Shahnazian, D., Silvetti, M., & Verguts, T. (2018). Human midcingulate cortex encodes distributed representations of task progress. *Proceedings of the National Academy of Sciences*, *115*(25), 6398–6403. https://doi.org/10.1073/pnas.1803650115

Hunt, L. T., Malalasekera, W. N., de Berker, A. O., Miranda, B., Farmer, S. F., Behrens, T. E., & Kennerley, S. W. (2018). Triple dissociation of attention and decision computations across prefrontal cortex. Nature neuroscience, 21(10), 1471-1481.

Huys, Q. J. M., Cools, R., Gölzer, M., Friedel, E., Heinz, A., Dolan, R. J., & Dayan, P. (2011). Disentangling the Roles of Approach, Activation and Valence in Instrumental and Pavlovian Responding. *PLOS Computational Biology*, *7*(4), e1002028. https://doi.org/10.1371/journal.pcbi.1002028

Jang, A. I., Sharma, R., & Drugowitsch, J. (2021). Optimal policy for attention-modulated decisions explains human fixation behavior. *eLife*, *10*, e63436. https://doi.org/10.7554/eLife.63436

Janiszewski, C., Kuo, A., & Tavassoli, N. T. (2013). The Influence of Selective Attention and Inattention to Products on Subsequent Choice. *Journal of Consumer Research*, *39*(6), 1258–1274. https://doi.org/10.1086/668234

Jiang, T., Potters, J., & Funaki, Y. (2016). Eye-tracking Social Preferences. *Journal of Behavioral Decision Making*, *29*(2–3), 157–168. https://doi.org/10.1002/bdm.1899

Johnson, J. G., & Busemeyer, J. R. (2005). A Dynamic, Stochastic, Computational Model of Preference Reversal Phenomena. *Psychological Review*, *112*(4), 841. https://doi.org/10.1037/0033-295X.112.4.841

Juechems, K., Balaguer, J., Ruz, M., & Summerfield, C. (2017). Ventromedial Prefrontal Cortex Encodes a Latent Estimate of Cumulative Reward. *Neuron*, *93*(3), 705-714.e4. https://doi.org/10.1016/j.neuron.2016.12.038

Kaanders, P., Nili, H., O'Reilly, J. X., & Hunt, L. (2021). Medial Frontal Cortex Activity Predicts Information Sampling in Economic Choice. *Journal of Neuroscience*, *41*(40), 8403–8413. https://doi.org/10.1523/JNEUROSCI.0392-21.2021

Kim, B., Seligman, D., & Kable, J. W. (2012). Preference Reversals in Decision Making Under Risk are Accompanied by Changes in Attention to Different Attributes. *Frontiers in Neuroscience*, *6*. https://doi.org/10.3389/fnins.2012.00109

Kleiner, M., Brainard, D., & Pelli, D. (2007). What's new in Psychtoolbox-3? *PERCEPTION*, *36*, 14–14.

Kolling, N., Wittmann, M. K., Behrens, T. E. J., Boorman, E. D., Mars, R. B., & Rushworth, M. F. S. (2016). Value, search, persistence and model updating in anterior cingulate cortex. *Nature Neuroscience*, *19*(10), Article 10. https://doi.org/10.1038/nn.4382

Konovalov, A., & Krajbich, I. (2016). Gaze data reveal distinct choice processes underlying model-based and model-free reinforcement learning. *Nature Communications*, *7*(1), Article 1. https://doi.org/10.1038/ncomms12438

Konovalov, A., & Krajbich, I. (2019). Revealed strength of preference: Inference from response times. *Judgment and Decision Making*, *14*(4), 381–394. Publicly Available Content Database.

Krajbich, I., Armel, C., & Rangel, A. (2010). Visual fixations and the computation and comparison of value in simple choice. *Nature Neuroscience*, *13*(10), 1292–1298. https://doi.org/10.1038/nn.2635

Krajbich, I., & Rangel, A. (2011). Multialternative drift-diffusion model predicts the relationship between visual fixations and choice in value-based decisions. *Proceedings of the National Academy of Sciences*, *108*(33), 13852–13857. https://doi.org/10.1073/pnas.1101328108

Levy, D. J., & Glimcher, P. W. (2011). Comparing Apples and Oranges: Using Reward-Specific and Reward-General Subjective Value Representation in the Brain. *Journal of Neuroscience*, *31*(41), 14693–14707. https://doi.org/10.1523/JNEUROSCI.2218-11.2011

Li, Z.-W., & Ma, W. J. (2021). An uncertainty-based model of the effects of fixation on choice. *PLOS Computational Biology*, *17*(8), e1009190. https://doi.org/10.1371/journal.pcbi.1009190

Lim, S.-L., O'Doherty, J. P., & Rangel, A. (2011a). The decision value computations in the vmPFC and striatum use a relative value code that is guided by visual attention. *Journal of Neuroscience*, *31*(37), 13214–13223. https://doi.org/10.1523/JNEUROSCI.1246-11.2011

Lim, S.-L., O'Doherty, J. P., & Rangel, A. (2011b). The Decision Value Computations in the vmPFC and Striatum Use a Relative Value Code That is Guided by Visual Attention. *Journal of Neuroscience*, *31*(37), 13214–13223. https://doi.org/10.1523/JNEUROSCI.1246-11.2011

Lopez-Persem, A., Domenech, P., & Pessiglione, M. (2016). How prior preferences determine decision-making frames and biases in the human brain. *eLife*, *5*, e20317. https://doi.org/10.7554/eLife.20317

MATLAB. (2016). R2016b. *The MathWorks Inc., Natick, Massachusetts*.

McGinty, V. B. (2019). Overt attention toward appetitive cues enhances their subjective value, independent of orbitofrontal cortex activity. *eNeuro*, *6*(6). https://doi.org/10.1523/ENEURO.0230-19.2019

McGinty, V. B., Rangel, A., & Newsome, W. T. (2016). Orbitofrontal cortex value signals depend on fixation location during free viewing. *Neuron*, *90*(6), 1299–1311. https://doi.org/10.1016/j.neuron.2016.04.045

Mullett, T. L., & Stewart, N. (2016). Implications of visual attention phenomena for models of preferential choice. *Decision*, *3*(4), 231. https://doi.org/10.1037/dec0000049

Mumford, J. A., Bissett, P. G., Jones, H. M., Shim, S., Rios, J. A. H., & Poldrack, R. A. (2024). The response time paradox in functional magnetic resonance imaging analyses. *Nature Human Behaviour*, *8*(2), 349–360. https://doi.org/10.1038/s41562-023-01760-0

Nichols, T. E., & Holmes, A. P. (2002). Nonparametric permutation tests for functional neuroimaging: A primer with examples. *Human Brain Mapping*, *15*(1), 1–25. https://doi.org/10.1002/hbm.1058

O'Connell, R. G., Shadlen, M. N., Wong-Lin, K., & Kelly, S. P. (2018). Bridging Neural and Computational Viewpoints on Perceptual Decision-Making. *Trends in Neurosciences*, *41*(11), 838–852. https://doi.org/10.1016/j.tins.2018.06.005

Orquin, J. L., & Mueller Loose, S. (2013). Attention and choice: A review on eye movements in decision making. *Acta Psychologica*, *144*(1), 190–206. https://doi.org/10.1016/j.actpsy.2013.06.003

Pärnamets, P., Johansson, P., Hall, L., Balkenius, C., Spivey, M. J., & Richardson, D. C. (2015). Biasing moral decisions by exploiting the dynamics of eye gaze. *Proceedings of the National Academy of Sciences*, *112*(13), 4170–4175. https://doi.org/10.1073/pnas.1415250112

Pelli, D. G. (1997). The VideoToolbox software for visual psychophysics: Transforming numbers into movies. *Spatial Vision*, *10*(4), 437–442. https://doi.org/10.1163/156856897X00366

Pisauro, M. A., Fouragnan, E., Retzler, C., & Philiastides, M. G. (2017). Neural correlates of evidence accumulation during value-based decisions revealed via simultaneous EEG-fMRI. *Nature Communications*, *8*(1), Article 1. https://doi.org/10.1038/ncomms15808

Pleskac, T. J., Yu, S., Grunevski, S., & Liu, T. (2022). Attention biases preferential choice by enhancing an option's value. *Journal of Experimental Psychology: General*. https://doi.org/10.1037/xge0001307

Polanía, R., Krajbich, I., Grueschow, M., & Ruff, C. C. (2014). Neural oscillations and synchronization differentially support evidence accumulation in perceptual and value-based decision making. *Neuron*, *82*(3), 709–720. https://doi.org/10.1016/j.neuron.2014.03.014

Polonio, L., Di Guida, S., & Coricelli, G. (2015). Strategic sophistication and attention in games: An eye-tracking study. *Games and Economic Behavior*, *94*, 80–96. https://doi.org/10.1016/j.geb.2015.09.003

Pooley, J. P., Lee, M. D., & Shankle, W. R. (2011). Understanding memory impairment with memory models and hierarchical Bayesian analysis. *Journal of Mathematical Psychology*, *55*(1), 47–56. https://doi.org/10.1016/j.jmp.2010.08.003

Ratcliff, R. (1978). A theory of memory retrieval. *Psychological Review*, *85*(2), 59.

Ratcliff, R., & Smith, P. L. (2004). A comparison of sequential sampling models for two-choice reaction time. *Psychological Review*, *111*(2), 333. https://doi.org/10.1037/0033-295X.111.2.333

Ratcliff, R., Smith, P. L., Brown, S. D., & McKoon, G. (2016). Diffusion Decision Model: Current issues and history. *Trends in Cognitive Sciences*, *20*(4), 260–281. https://doi.org/10.1016/j.tics.2016.01.007

Rich, E. L., & Wallis, J. D. (2016). Decoding subjective decisions from orbitofrontal cortex. *Nature Neuroscience*, *19*(7), Article 7. https://doi.org/10.1038/nn.4320

Rodriguez, C. A., Turner, B. M., Zandt, T. V., & McClure, S. M. (2015). The neural basis of value accumulation in intertemporal choice. *European Journal of Neuroscience*, *42*(5), 2179–2189. https://doi.org/10.1111/ejn.12997

Roe, R. M., Busemeyer, J. R., & Townsend, J. T. (2001). Multialternative decision field theory: A dynamic connectionst model of decision making. *Psychological Review*, *108*(2), 370–392. https://doi.org/10.1037/0033-295X.108.2.370

Rouault, M., Drugowitsch, J., & Koechlin, E. (2019). Prefrontal mechanisms combining rewards and beliefs in human decision-making. *Nature Communications*, *10*(1), Article 1. https://doi.org/10.1038/s41467-018-08121-w

Russo, J. E., & Leclerc, F. (1994). An Eye-Fixation Analysis of Choice Processes for Consumer Nondurables. *Journal of Consumer Research*, *21*(2), 274–290. https://doi.org/10.1086/209397

Sepulveda, P., Usher, M., Davies, N., Benson, A. A., Ortoleva, P., & De Martino, B. (2020). Visual attention modulates the integration of goal-relevant evidence and not value. *eLife*, *9*, e60705. https://doi.org/10.7554/eLife.60705

Shadlen, M. N., & Shohamy, D. (2016). Decision making and sequential sampling from memory. *Neuron*, *90*(5), 927–939. https://doi.org/10.1016/j.neuron.2016.04.036

Sheng, F., Ramakrishnan, A., Seok, D., Zhao, W. J., Thelaus, S., Cen, P., & Platt, M. L. (2020). Decomposing loss aversion from gaze allocation and pupil dilation. *Proceedings of the National Academy of Sciences*, *117*(21), 11356–11363. https://doi.org/10.1073/pnas.1919670117

Shenhav, A., Straccia, M. A., Botvinick, M. M., & Cohen, J. D. (2016). Dorsal anterior cingulate and ventromedial prefrontal cortex have inverse roles in both foraging and economic choice. *Cognitive, Affective, & Behavioral Neuroscience*, *16*(6), 1127–1139. https://doi.org/10.3758/s13415-016-0458-8

Shenhav, A., Straccia, M. A., Cohen, J. D., & Botvinick, M. M. (2014). Anterior cingulate engagement in a foraging context reflects choice difficulty, not foraging value. *Nature Neuroscience*, *17*(9), Article 9. https://doi.org/10.1038/nn.3771

Shi, S. W., Wedel, M., & Pieters, F. G. M. (Rik). (2012). Information Acquisition During Online Decision Making: A Model-Based Exploration Using Eye-Tracking Data. *Management Science*, *59*(5), 1009–1026. https://doi.org/10.1287/mnsc.1120.1625

Shimojo, S., Simion, C., Shimojo, E., & Scheier, C. (2003). Gaze bias both reflects and influences preference. *Nature Neuroscience*, *6*(12), Article 12. https://doi.org/10.1038/nn1150

Smith, S. M., & Krajbich, I. (2018). Attention and choice across domains. *Journal of Experimental Psychology: General*, *147*(12), 1810–1826. https://doi.org/10.1037/xge0000482

Smith, S. M., & Krajbich, I. (2019). Gaze Amplifies Value in Decision Making. *Psychological Science*, *30*(1), 116–128. https://doi.org/10.1177/0956797618810521

Smith, S. M., Krajbich, I., & Webb, R. (2019). Estimating the dynamic role of attention via random utility. *Journal of the Economic Science Association*, *5*(1), 97–111. https://doi.org/10.1007/s40881-019-00062-4

Stewart, N., Hermens, F., & Matthews, W. J. (2016). Eye movements in risky choice. *Journal of Behavioral Decision Making*, *29*(2–3), 116–136. https://doi.org/10.1002/bdm.1854

Tavares, G., Perona, P., & Rangel, A. (2017). The attentional drift diffusion model of simple perceptual decision-making. *Frontiers in Neuroscience*, *11*. https://doi.org/10.3389/fnins.2017.00468

Teoh, Y. Y., Yao, Z., Cunningham, W. A., & Hutcherson, C. A. (2020). Attentional priorities drive effects of time pressure on altruistic choice. *Nature Communications*, *11*(1), 3534. https://doi.org/10.1038/s41467-020-17326-x

Thomas, A. W., Molter, F., Krajbich, I., Heekeren, H. R., & Mohr, P. N. C. (2019). Gaze bias differences capture individual choice behaviour. *Nature Human Behaviour*, *3*(6), Article 6. https://doi.org/10.1038/s41562-019-0584-8

Towal, R. B., Mormann, M., & Koch, C. (2013). Simultaneous modeling of visual saliency and value computation improves predictions of economic choice. *Proceedings of the National Academy of Sciences of the United States of America*, *110*(40), E3858–E3867. https://doi.org/10.1073/pnas.1304429110

Tsetsos, K., Chater, N., & Usher, M. (2012). Salience driven value integration explains decision biases and preference reversal. *Proceedings of the National Academy of Sciences*, *109*(24), 9659–9664. https://doi.org/10.1073/pnas.1119569109

Usher, M., & McClelland, J. L. (2001). The time course of perceptual choice: The leaky, competing accumulator model. *Psychological Review*, *108*(3), 550.

Vaidya, A. R., & Fellows, L. K. (2015). Testing necessary regional frontal contributions to value assessment and fixation-based updating. *Nature Communications*, *6*(1), Article 1. https://doi.org/10.1038/ncomms10120

Vanunu, Y., Hotaling, J. M., Le Pelley, M. E., & Newell, B. R. (2021). How top-down and bottom-up attention modulate risky choice. *Proceedings of the National Academy of Sciences*, *118*(39), e2025646118. https://doi.org/10.1073/pnas.2025646118

Vassena, E., Deraeve, J., & Alexander, W. H. (2020). Surprise, value and control in anterior cingulate cortex during speeded decision-making. *Nature Human Behaviour*, *4*(4), Article 4. https://doi.org/10.1038/s41562-019-0801-5

Venkatraman, V., Payne, J. W., & Huettel, S. A. (2014). An overall probability of winning heuristic for complex risky decisions: Choice and eye fixation evidence. *Organizational Behavior and Human Decision Processes*, *125*(2), 73–87. https://doi.org/10.1016/j.obhdp.2014.06.003

Wang, J. T., Spezio, M., & Camerer, C. F. (2010). Pinocchio's Pupil: Using Eyetracking and Pupil Dilation to Understand Truth Telling and Deception in Sender-Receiver Games. *American Economic Review*, *100*(3), 984–1007. https://doi.org/10.1257/aer.100.3.984

Wang, X.-J. (2002). Probabilistic Decision Making by Slow Reverberation in Cortical Circuits. *Neuron*, *36*(5), 955–968. https://doi.org/10.1016/S0896-6273(02)01092-9

Westbrook, A., van den Bosch, R., Määttä, J. I., Hofmans, L., Papadopetraki, D., Cools, R., & Frank, M. J. (2020). Dopamine promotes cognitive effort by biasing the benefits versus costs of cognitive work. *Science*, *367*(6484), 1362–1366. https://doi.org/10.1126/science.aaz5891

Wittmann, M. K., Fouragnan, E., Folloni, D., Klein-Flügge, M. C., Chau, B. K. H., Khamassi, M., & Rushworth, M. F. S. (2020). Global reward state affects learning and activity in raphe nucleus and anterior insula in monkeys. *Nature Communications*, *11*(1), Article 1. https://doi.org/10.1038/s41467-020-17343-w

Wittmann, M. K., Kolling, N., Akaishi, R., Chau, B. K. H., Brown, J. W., Nelissen, N., & Rushworth, M. F. S. (2016). Predictive decision making driven by multiple time-linked

reward representations in the anterior cingulate cortex. *Nature Communications*, *7*(1), Article 1. https://doi.org/10.1038/ncomms12327

Yang, T., & Shadlen, M. N. (2007). Probabilistic reasoning by neurons. *Nature*, *447*(7148), Article 7148. https://doi.org/10.1038/nature05852

Yang, X., & Krajbich, I. (2023). A dynamic computational model of gaze and choice in multi-attribute decisions. *Psychological Review*, *130*(1), 52–70. https://doi.org/10.1037/rev0000350

Zilker, V., & Pachur, T. (2023). Attribute attention and option attention in risky choice. *Cognition*, *236*, 105441. https://doi.org/10.1016/j.cognition.2023.105441

Zilker, V., & Pachur, T. (2023). Nonlinear probability weighting can reflect attentional biases in sequential sampling. *Psychological Review*, *129*(5), 949.